scientific reports

Check for updates

OPEN

Exploring marine-derived bacterial compounds targeting the μ-opioid receptor agonists through metabolic profiling to molecular modeling

Daouia Boudrahem[1], Omar Messaoudi[2,3,4], Sarah Balit[1], Mouloud Kecha[1], Joachim Wink[5] & Chirag N. Patel[6,7,8]✉

Given the severe side effects of prolonged morphine use, the search for safer alternatives is a global priority. This study investigates marine bacteria from sediments along the Bejaia coast, Algeria, to identify opioid-like bioactive compounds with potential analgesic properties. A total of 45 bacterial strains were isolated using six different culture media, with 18 strains exhibiting antimicrobial activity. Molecular identification based on 16S rRNA gene sequencing classified these strains into six genera: *Streptomyces*, *Nocardiopsis*, *Alloalcanivorax*, *Pseudonocardia*, *Sinomicrobium*, and *Lysinibacillus*. One strain, S5T2H1, was identified as a new *Streptomyces* species through a polyphasic approach. LC-HRESIMS analysis of secondary metabolites revealed that strain S56T3J31 produced A58365A, antimycin A, and three potentially novel compounds. However, strain S5T2H1 synthesized cyclo(phenylalanyl-prolyl) and niphimycin Ia, along with three unidentified metabolites, while strain S7T2H1 secreted a single compound identified as berberifuranol. Molecular docking and molecular dynamics simulations demonstrated that A58365A exhibited strong interactions with the μ-opioid receptor (5C1M), showing a stable binding affinity comparable to morphine. These findings highlight marine-derived bacterial compounds as promising candidates for opioid drug development.

Keywords Isolation, Marine-derived bacteria, Marine sediment, μ-opioid receptor, Metabolic profiling, Molecular modeling

The opioid drugs, such as morphine, heroin, and fentanyl, are widely used as potent analgesics for managing moderate to severe pain[1]. In addition to their primary role in pain relief, these drugs are also utilized in other medical applications, including the treatment of drug dependence[2]. Morphine, the prototypical opioid, is a naturally occurring alkaloid derived from the opium poppy (*Papaver somniferum*)[3]. It exerts its analgesic effects by binding activating the μ-opioid receptor, which is primarily located in the nervous system. This interaction triggers a cascade of physiological responses, ultimately leading to pain relief[4]. However, prolonged use of morphine is associated with severe side effects, including respiratory depression, sedation, constipation, and nausea[5]. As a result, morphine-related deaths have risen dramatically in recent years.

Given these challenges, the search for alternative analgesics that retain the therapeutic efficacy of morphine while minimizing its adverse effects has become a global priority. In this context, marine environments have emerged as a valuable source of bioactive secondary metabolites with diverse pharmacological activities[6].

[1]Université de Bejaia, Faculté des Sciences de la Nature et de la Vie, Laboratoire de Microbiologie Appliquée, Bejaia 06000, Algeria. [2]Laboratory of Applied Microbiology in Food, Biomedical and Environment, Abou Bekr Belkaïd University, 13000 Tlemcen, Algeria. [3]Department of Biology, Faculty of Science, University of Amar Telidji, 03000 Laghouat, Algeria. [4]Research Unit of Medicinal Plant (RUMP) Attached to Center of Biotechnology (CRBt, 3000, Constantine), 03000 Laghouat, Algeria. [5]Microbial Strain Collection, Helmholtz Centre for Infection Research GmbH (HZI), Inhoffenstrasse 7, 38124 Brunswick, Germany. [6]Department of Botany, Bioinformatics & Climate Impacts Management, University School of Sciences, Gujarat University, Navrangpur, Ahmedabad 280009, Gujarat, India. [7]Biotechnology Research Center, Technology Innovation Institute, 9639 Abu Dhabi, United Arab Emirates. [8]Drug Design & Development Section, Translational Gerontology Branch, Intramural Research Program, National Institute on Aging, NIH, Baltimore, MD 21224, USA. ✉email: chiragpatel269@gmail.com

Notably, several marine-derived compounds have demonstrated opioid-like activity, presenting promising leads for the development of safer analgesics[7].

Among these marine ecosystems, the Algerian coast, which forms part of the larger Mediterranean coastline, spans approximately 1600 km from the western border of Tunisia to the eastern border of Morocco[8]. This region harbors a wealth of untapped habitats that support unique microbial communities, many of which remain largely unexplored[9]. Due to the specific and diverse microclimatic conditions of these coastal environments, some microbial species found in these regions may be endemic[10]. Therefore, exploring marine microorganisms isolated from Algerian coastal ecosystems could lead to the discovery of novel, safer alternatives to conventional opioid drugs, offering a potential solution to the severe side effects associated with morphine. In this context, this study focuses on culturable bacteria from marine sediments along the Bejaia coastline (Algeria) to identify bioactive compounds with pharmaceutical relevance as potential alternatives to morphine. The main goals of this study were to: (i) Investigate the biodiversity of culturable bacteria isolated from marine sediments collected from the Bejaia coastline (Algeria). (ii) Assess their antimicrobial potential against various target microorganisms, in order to select the potent strains. (iii) Identify and annotate secondary metabolites from the selected strains using High-Performance Liquid Chromatography coupled with High-Resolution Mass Spectrometry (HPLC-ESI-HRMS), and. (iv) Exploring the identified marine-derived compounds secreted by selected marine bacterial strains as potential alternatives to morphine, through in silico approaches, including docking studies, molecular dynamics simulations and MM/GBSA binding free energy calculations.

Materials and methods

Sampling of marine sediments

The isolation of marine bacterial strains was carried out from marine sediments samples collected from four different sites, located on the west coast of Bejaia, Algeria: Tazboujth (36°48′13 0.96″N and 5°00′52.17″E), Cap Sigli (36°53′52 0.65″N and 4°45′31.00″E), fishing port (36°49′31.68″N and 4°56′ 49.97″E), Saket (36°49′50 0.44″N and 4°56′10.35″E). The samples were collected at a depth of 2 to 3 m, packed in sterile bags, and stored at 4 °C for further analysis.

Determination of physicochemical properties of sediments

The physicochemical parameters of the sediments, including pH, salinity (g/L), and organic matter (%), were analyzed for each sediment sample collected from Tazeboujth, Port de Pêche, Saket, and Cap Sigli in Bejaia, Algeria. pH was measured using a pH meter (Hanna HI5120), and salinity was determined using an electrical conductivity meter (Hanna HI5120). However, organic matter content was determined by drying the samples at 100 °C for 24 h, followed by ashing at 550 °C, with calculations based on weight loss. Peat humification was assessed using the method of Schumacher[11].

Isolation of marine bacterial strains

The marine sediment samples were air-dried at room temperature to reduce moisture content and eliminate fast-growing, non-spore-forming bacteria. One gram of each dried sediment sample was diluted in 3 mL of sterile seawater (dilution 1/3) to resuspend microbial cells while maintaining osmotic balance. This was followed by moderate heat treatment at 55 °C for 6 min to selectively enrich heat-resistant and spore-forming bacteria, such as actinobacteria and certain *Bacillaceae* members[12]. An aliquot of 100 µL was taken from this suspension and spread in duplicate on agar plates containing six different media: Casein Starch Agar (SCA)[13], Marine 2 Medium (M2)[14], NaST21Cx Agar[15], Nutrient-Poor Sediment Medium (NPS), Nutrient-Rich Sediment Medium (NRS), and Selective Mannitol Peptone Medium (SMP)[12], each designed to support the growth of diverse marine bacterial taxa with potential bioactive metabolite production.

Screening for antimicrobial activity of marine bacterial strains

Preparation of bacterial suspension

The antibacterial activity of the marine bacterial strains was evaluated against nine pathogenic bacterial species. Among them, five Gram-positive bacteria, including *Staphylococcus aureus* ATCC 25923, methicillin-resistant *Staphylococcus aureus* (MRSA) ATCC 43300, *Listeria innocua* CLIP 74915, *Bacillus subtilis* and *Enterococcus faecalis*, were tested. Similarly, four Gram-negative bacteria were also assessed: *Escherichia coli* ATCC 25922, *Klebsiella pneumoniae* ATCC 700603, *Pseudomonas aeruginosa* ATCC 27853, and *Proteus* sp. It is worth mentioning that two of the tested strains, *Enterococcus faecalis* and *Proteus* sp., were obtained from the University Hospital Center Khellil AMRANE in Bejaia, having been isolated from clinical samples collected from patients. Furthermore, the antifungal activity was tested against nine microscopic fungi, including seven filamentous fungi, such as *Aspergillus niger* 939N, *Aspergillus carbonarius* A731C, *Aspergillus flavus* NRRL, *Aspergillus ochraceus* NRRL3174, *Aspergillus parasiticus* CB5, *Mucor rammanianus* NRRL 1829, *Fusarium polyferatum*, *Botrytis cinerea*, and one yeast, *Candida albicans*.

To prepare microbial suspensions, the tested bacterial strains were inoculated into nutrient broth and incubated at 37 °C for 18 h. However, the yeast *Candida albicans* was seeded in MYG medium (1.0% phytone peptone, 1.0% glucose, 50 mM HEPES [11.9 g/L], pH 7.0) and incubated at 30 °C for 48 h. In addition, the tested microscopic filamentous fungi were grown in Malt Extract Agar (MEA) at 25 °C for 5 days.

For each tested bacterial and yeast suspension, the turbidity was adjusted to 0.5 McFarland and 0.1 McFarland, respectively, measured at 600 nm using a Shimadzu UV spectrophotometer 1240. However, for the tested microscopic fungi, spore suspensions were adjusted to 10^7 spores/mL in physiological saline using a hemocytometer[16]. This standardized suspension was then utilized in subsequent antimicrobial activity assays.

Antimicrobial activity of marine bacterial strains

The marine bacteria isolates were inoculated on 5294 plates medium (Glucose: 15.0 g/l; Soymeal 15.0 g/l; Corn steep 5.0 g/l; $CaCO_3$ 2.0 g/l; NaCl 5.0 g /l; Eau distillée: 1000 ml. pH = 7.2), and incubated at 30 °C for 14 days. The antibacterial activity of marine bacteria strains was evaluated by agar cylinder method. 6 mm cylinders were cut from the well-developed culture of bacteria strains and then placed on the surface of Muller Hinton medium for bacteria[17], MYG for yeast and MEA medium for microscopic filamentous fungi[18], already seeded with test microorganisms. The plates were maintained at 4 °C for 4 h to ensure good diffusion of bioactive compounds secreted by bacteria strains, followed by incubation to the suitable temperature. The inhibition areas were measured after 24 h (bacteria and yeasts) and 48 h (microscopic fungi)[19].

Molecular identification of active marine bacterial strains

The genomic DNA of bacteria strains has been extracted using Invisorb Spin Plant Mini Kit (Invitek. GmbH, Berlin, Germany), following the manufacturer's protocol. The quality of the achieved DNA was checked via an 0.8% agarose gel electrophoresis. The 16S rRNA gene region was amplified through PCR with 2 universal primers on the positions 27F (AGA GTT TGA TCC TGG CTC AG) and 1525R (AAG GAG GTG WTC CAR CC). The PCR reaction was conducted using a special master mix containing primers, PCR water and "Jump Start Ready Mix (JSRM)" including, 99% pure deoxynucleotides, JumpStart Taq DNA polymerase, and buffer in an optimized reaction concentrate[20].

The PCR reaction was performed in 200 µL microtubes containing: 22 µl PCR water, 25 µl JSRM, 1 µl reverse and forward primer dilution as well as 1 µl of the template DNA. One tube remains without DNA and therefore serves as control. The PCR reaction was conducted in a Mastercycler Gradient (Eppendorf, Hambourg, Germany) under the program: Initial denaturation at 95 °C for 5 min, 35 cycles of denaturation at 94 °C for 30 s, annealing at 52 °C for 30 s, elongation at 72 °C for 120 s, and a final extension at 72 °C for 10 min. Before 16S rRNA sequencing, the PCR products have been purified from the reaction residues using NucleoSpin® Gel and PCR Clean-up kit (MachereyNagel, Düren, Germany). The success of the PCR was checked by electrophoresis. 16S rRNA genes of bacteria strains were sequenced using two primers such as 27F and R518[8].

The obtained sequences were checked for quality and assembled using the program "Bioedit alignment, v 7.0.5.3". The obtained sequences were compared to an online databank using the "Basic Local Alignment Search Tool" (BLAST) of the National Center for Biotechnology Information (NCBI)[20]. Selected strains, which exhibited low percentages of similarity with the closest type species, were subjected to morphological, physiological, and biochemical characterization. The results were compared to the closest species described in the *Compendium of Actinobacteria*: https://www.dsmz.de/collection/catalogue/microorganisms/special-groups-of-organisms/compendium-of-actinobacteria.

Cultural characteristics were determined according to the methods described by Shirling and Gottlieb[21]. Physiological characterization, including growth at different temperatures and NaCl concentrations, was assessed using GYM medium as the basal medium after two weeks of incubation. The ability of the selected strains to utilize ten different carbon sources (glucose, arabinose, sucrose, xylose, inositol, mannose, fructose, rhamnose, raffinose, cellulose) was tested at 30 °C, following the methods outlined by Shirling and Gottlieb[21]. Enzymatic activities, including nitrate reductase, urease, gelatin liquefaction, and H_2S production, were determined using API® CORYNE, API® CAMPY, and API® Zym test strips (bioMérieux, Marcy-l'Étoile, France).

HPLC–UV-HRMS analysis of crude extracts from selected marine bacterial strains

Bioactive compounds in crude extracts from selected marine bacterial strains were annotated and identified through analysis using HPLC [Agilent 1260 series RP-HPLC system: column 50 × 2.1 mm Acquity UPLC BEH C_{18} (Waters); solvent A: 0.1% formic acid in H_2O, B: 0.1% formic acid in acetonitrile; gradient system: 5% B for 0.5 min, in 19.5 min to 100% B and maintained for 5 min at 100% B; flow rate 0.6 mL/min; 40 °C; DAD-UV detection at 200–600 nm], coupled to mass spectrometry, High resolution electrospray ionization mass spectrometry (HRESIMS), data were recorded on a MaXis ESI-TOF-mass spectrometer (Bruckers Daltonics). Molecular formulas were calculated including the isotopic pattern with the Smart Formula algorithm (Bruckers). Comparison of results was performed by Dictionary of Natural Product. Compounds annotation were only be concluded if the respective mass shown distinctive molecular ion cluster ($[M+H]^+$, $[M+Na]^+$, $[2M+H]^+$, or $[2M+Na]^+$.

In silico study

Molecular docking

The Glide program, part of the Schrödinger suite and enhanced with Extra Precision (XP) capabilities, was used to attach ligands into the crystal structure of the mu-upload receptor in association with the BU72 agonist protein. XP docking, which is more thorough and selective than the standard precision (SP) technique, takes longer due to its complex methodology. It is designed for ligands that have already obtained high scores in SP docking, and it uses a comprehensive scoring methodology that requires stronger compatibility between ligand and receptor geometries. This meticulous process aims to eliminate the false positives often encountered with SP, by imposing penalties on ligands that poorly match the chosen receptor conformation[22]. To perform the molecular docking both the receptor (Crystal structure of active mu-opioid receptor bound to the agonist BU72 with 5C1M PDB) and ligands, were prepared through addition of hydrogen, removal of water molecules and energy minimization. The active site of the receptor was identified via existing binding affinity of 4VO ((2S,3S,3aR,5aR,6R,11bR,11cS)-3a-methoxy-3,14-dimethyl-2-phenyl-2,3,3a,6,7,11c-hexahydro-1H-6,11b-(epiminoethano)-3,5a-m ethanonaphtho[2,1-g]indol-10-ol). As a result, docking against numerous receptor conformations is advised in order to find ligands with appropriate binding energies for molecular dynamic simulation analysis.

Molecular dynamics simulations

The Desmond software, version 2.0 (Schrödinger Release 2024-4) https://www.schrodinger.com/platform/products/desmond/, was used to evaluate the stability of receptor-ligand complexes generated by molecular docking[23–27]. The simulation setup included the TIP3P water model within a cubic periodic box measuring 10 Å on each side, utilizing the Simple Point Charge (SPC) technique, combined with the OPLS all-atom force field from 2005[28]. To achieve charge neutrality, sodium ions were introduced. A number of regulated processes were used to reduce the energy of the complexes and prepare them for equilibrium. Molecular dynamics (MD) simulations were run using periodic boundary conditions, using the OPLS 2005 force field parameters, a 1 ps relaxation duration, and a constant temperature of 300 K and volume in the NPT ensemble[29]. To achieve charge neutrality, sodium ions were introduced. A number of regulated processes were used to reduce the energy of the complexes and prepare them for equilibrium. Molecular dynamics (MD) simulations were run using periodic boundary conditions, using the OPLS 2005 force field parameters, a 1 ps relaxation duration, and a constant temperature of 300 K and volume in the NPT ensemble.

MM-GBSA (molecular mechanics generalized born surface area) binding energies

The MM-GBSA and MM-PBSA approaches were used to calculate the binding free energies of protein–ligand complexes. The PRIME module in Maestro 11.4, together with the OPLS-2005 force field, was utilized to calculate the binding energies of the ideally docked ligand-receptor couples. The binding energy is calculated using a particular formula:

$$\Delta G_{Bind} = \Delta E_{MM} + \Delta G_{Solv} + \Delta G_{SA}$$

where ΔEMM denotes the energy difference after minimization of the protein–ligand complex, ΔGSolv is the discrepancy in GBSA solvation energy between the complex and the individual protein and ligand energies, and ΔGSA refers to the change in surface area energies within the protein–ligand complex compared to the sum of their separate surface energies. The minimization of the protein–ligand complexes was achieved through the local optimization feature in PRIME[30].

Results and discussion

Physicochemical analysis of marine sediment

The physicochemical analysis, presented in Supplementary Table S1, includes pH, salinity, and organic matter, was conducted for four marine sediment samples collected from different regions of Bejaia, Algeria. These parameters are key environmental factors influencing microbial diversity[31]. Results indicated that all sites exhibited alkaline conditions (pH 7.78–8.13), likely due to carbonate-rich coastal sediments, which can support alkaliphilic bacteria. However, Tazeboujth had the lowest salinity (0.468 g/L) and organic matter content (1.07%), which may limit microbial diversity due to nutrient scarcity. In contrast, Saket (8.248 g/L) and Cap Sigli (7.216 g/L) exhibited high salinity and organic matter content, potentially favoring halotolerant microbial communities[32]. These findings suggest that each site harbors a distinct microbial ecosystem shaped by variations in acidity/alkalinity, salinity, and nutrient availability. The interplay between these factors likely influences the composition and adaptability of microbial communities in each marine sediment[32,33].

Isolation of marine bacterial strains

The investigation of microbial diversity in marine sediment collected from four different sites in the Bejaia region, Algeria, using different culture media led to the isolation of 45 distinct marine strains, selected based on their diverse morphological characteristics (Supplementary Fig. S1). Exploring the microbial diversity of the underexplored Algerian coast presents a unique opportunity to identify potent marine-derived compounds targeting the μ-opioid receptor, potentially providing innovative scaffolds for safer and more effective analgesics[4,6]. To date, few studies have investigated bacterial diversity in this region, making our findings valuable for expanding the current understanding of marine microbial communities in Algeria[8,9].

The comparison between the efficiency of the culture media used indicates that Casein Starch Agar (SCA)[13,34] was the most effective medium for isolating bacteria from marine sediments collected in the Bejaia region, Algeria (Fig. 1). A total of 24 isolates were obtained using this medium, while 14 isolates were recovered from M2[14], 5 from NaST21Cx[15], and 2 from NRS[6]. No isolates were obtained using NPS or SMP media[12]. This difference could be explained by the presence of starch and casein in SCA medium, which stimulate the growth of several bacteria, including actinomycetes[19]. Several studies have confirmed that this medium is effective for the selective isolation of bacteria from various ecosystems[35–39].

Media with a low concentration of organic nutrients, such as NPS and NRS, delay the growth of fast-growing bacteria for a sufficient period, enabling slow-growing bacteria to emerge[40]. However, in our case, we were only able to obtain two isolates using NRS. Different pretreatment procedures and selective isolation media are recommended for the isolation of marine bacteria, such as Actinobacteria. There is no universal isolation technique, but it is always necessary to vary the methods and media in the same screening[41].

Screening for antimicrobial activity

Antibacterial activity

The antibacterial activity of the 45 marine bacterial strains was assessed against four Gram-negative and five Gram-positive bacteria, with the results presented in Supplementary Table S2. Among the 45 tested isolates, 11 strains exhibited antimicrobial activity against at least one tested bacterium. Among them, three strains demonstrated activity exclusively against Gram-positive bacteria, while two strains showed activity only against Gram-negative bacteria. Additionally, six strains displayed activity against both Gram-positive and Gram-

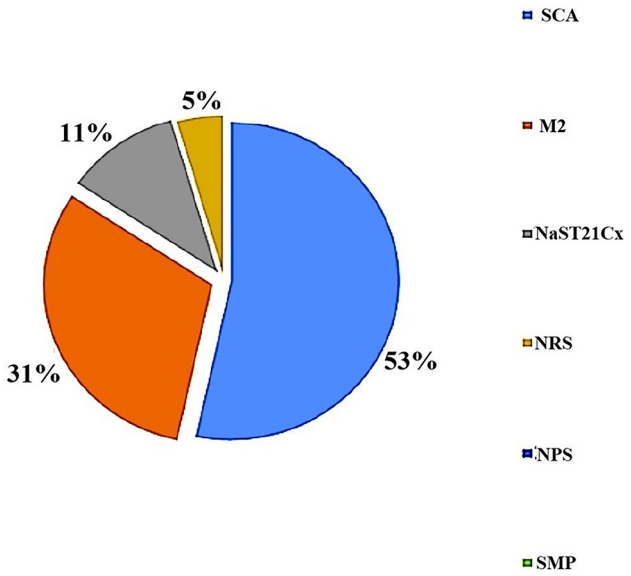

Fig. 1. Distribution of the number of bacteria isolates according to the culture medium.

negative bacteria. Among the marine bacterial isolates, strain S5T2H1 was the most active, exhibiting significant inhibition zones, particularly against Gram-positive bacteria. It showed an inhibition zone of 35 mm against *Staphylococcus aureus*, 30 mm against both MRSA and *Enterococcus faecalis*, and 28 mm against *Listeria innocua*. Additionally, this strain demonstrated activity against the Gram-negative bacterium *Pseudomonas aeruginosa*, with an inhibition zone of 23 mm (Supplementary Fig. S2).

Regarding the resistance of the tested bacteria, both *K. pneumoniae* and *Proteus* sp. exhibited the highest resistance, as none of the marine bacterial strains showed activity against them. In contrast, *Bacillus cereus* was the most susceptible. The susceptibility of Gram-positive bacteria to the bioactive compounds secreted by marine bacterial strains, compared to Gram-negative bacteria, may be attributed to differences in their cell wall structure. The presence of lipopolysaccharides in the outer membrane of Gram-negative bacteria reduces permeability to lipophilic compounds, making them more resistant[42].

The stronger the antimicrobial activity exhibited by the marine bacterial strains, the more it suggests that these isolates secrete a diverse array of bioactive compounds, potentially extending beyond antibacterial properties to include metabolites with pharmacological potential[43–45]. Therefore, given that many secondary metabolites from marine microorganisms interact with human receptors, the marine strains isolated from the Algerian coast could serve as a valuable source of novel compounds for targeting the μ-opioid receptor, providing promising scaffolds for the development of safer and more effective analgesics[46,47].

Antifungal activity

The antifungal activity of the 45 marine bacterial strains was evaluated against eight filamentous fungi and one yeast. The results are presented in Supplementary Table S3. The results indicate that eleven strains exhibited antifungal activity against at least one of the eight tested filamentous fungi (Supplementary Fig. S3). Among these, S5T2H1 was the most active strain, exhibiting potent antifungal activity against five tested filamentous fungi, along with the yeast Candida albicans, with inhibition diameters ranging from 13 to 35 mm (Supplementary Fig. S3). Additionally, *Candida albicans* exhibited greater sensitivity to the bioactive compounds secreted by marine actinomycete strains compared to the tested filamentous fungi, as indicated by the inhibition zones ranging from 15 to 28 mm (Supplementary Fig. S3).

Marine bacteria are a valuable resource for drug discovery against various diseases[48,49]. Therefore, the antifungal activity of the secondary metabolites secreted by marine bacteria isolated from the Algerian littoral suggests their ability to interact with eukaryotic cells, such as filamentous fungi and *Candida albicans*. This indicates that these marine strains could be promising candidates for producing compounds that may interact with the human μ-opioid receptor, offering potential scaffolds for the development of new analgesics[50,51].

Molecular identification and phylogenetic study of selected actives strains

The eighteen marine bacterial strains, selected from the 45 obtained isolates for their significant antimicrobial activity, were subjected to molecular identification based on 16S rRNA gene sequencing, as they could be promising candidates for producing compounds that may interact with the human μ-opioid receptor. The obtained sequences were compared to the closest homologs registered in the GenBank database using the BLAST tool, with the results presented in Supplementary Table S2. The results revealed that the identified isolates belong to six different genera, including seven *Streptomyces* strains, six *Nocardiopsis* strains, and three strains each affiliated with *Alloalcanivorax* and *Pseudonocardia*. Additionally, a single strain was identified as *Sinomicrobium*, and another as *Lysinibacillus*.

Among the identified strains, four *Nocardiopsis* isolates were assigned to *N. terra* (S29T3J31, S57T3J31; 99.65–99.70% similarity) and *N. umidischolae*/*N. alborubida* (S3T3I1, S7T2H1; 99.40% similarity) (Supplementary Table S4). Three strains (S5T3I1, S1T2Kmr, S6T3I1) showed high similarity to *Pseudonocardia* species (99.80–100%), supported by strong phylogenetic bootstrap values (Fig. 2). Additionally, two strains, S1PHmr, S1PKmr, were related to the species *Streptomyces antimycoticus* and *Streptomyces aculeolatus*, respectively, with 100% similarity. Meanwhile, strains S56T3J31, S2T2H1, and S6T2H1 were identified as *S. humidus, S. albogriseolus,* and *S. chitinivorans,* respectively, with 99.30–99.75% similarity.

Phylogenetic analysis confirmed the molecular identification of S37T3J31 and S28T3J31, clustering them with *Sinomicrobium oceani* (99.90% similarity) and *Lysinibacillus fusiformis* (99.80%) (Fig. 2, Supplementary Table S4). Additionally, *Alloalcanivorax* strains S1T3J31, S4T3I1, and S2T3I1 formed a stable phylogenetic clade with *A. dieselolei, A. balearicus*, and *A. xenomutans* (Fig. 2). The Actinobacteria genera *Streptomyces* and *Nocardiopsis* have been previously reported in Algerian marine environments. However, this study marks the first isolation of *Pseudonocardia, Sinomicrobium, Alloalcanivorax*, and *Lysinibacillus* from Algerian marine sediments[8,52]. The latter three genera have been previously found in deep-sea sediments[53,54], methane cold seep sites[55,56], and tidal flats[57,58].

One strain, S5T2H1, shares 98.5% 16S rRNA gene sequence similarity with *Streptomyces coelicoflavus*, which is below the threshold for differentiating between bacterial species. According to Kim et al.[59], this threshold is set at 98.65%, meaning that strains with lower similarity are likely considered different species. Fourthermore, the phylogenetic analysis (Fig. 2) demonstrated that this strain forms a stable and distinct lineage separate from neighboring species within the tree (bootstrap value > 80%). Therefore, it may represent a new species within the genus *Streptomyces*. However, to better differentiate strain S5T2H1 from its closest phylogenetic neighbors, *Streptomyces antimycoticus* and *Streptomyces aculeolatus*, additional characterization was conducted, with the main differences highlighted in Supplementary Table S5.

Several macromorphological differences were observed between strain S5T2H1 and its closest species, *Streptomyces coelicoflavus* and *Streptomyces fragilis* (Supplementary Table S5). The aerial mycelium of strain S5T2H1 appeared pebble grey on ISP2, white on ISP3, ISP4, and ISP5, and was absent on ISP6 and ISP7. In contrast, *Streptomyces coelicoflavus* formed aerial mycelium only on ISP3 and ISP4, with a window grey color. Meanwhile, the aerial mycelium of *Streptomyces fragilis* ranged from grey on ISP2, ISP3, and ISP6, to white on ISP4 and ISP5. The differences between strain S5T2H1 and its two closest species extend to biochemical characteristics. Strain S5T2H1 was able to utilize all the tested carbon sources except lactose. In contrast, *Streptomyces coelicoflavus* could not utilize xylose and succinate, while *Streptomyces fragilis* exhibited a limited metabolic profile, utilizing only three carbon sources: D-galactose, L-arabinose, and sucrose. Additionally, *Streptomyces fragilis* was the only species that exhibited gelatin liquefaction (Supplementary Table S5).

Based on the results of molecular identification, phylogenetic studies, and the observed morphological and biochemical differences from *Streptomyces coelicoflavus* and *Streptomyces fragilis*, strain S5T2H1 is a strong candidate to be a new species within the genus *Streptomyces*. However, further investigation, including whole-genome sequencing and digital DNA-DNA hybridization (dDDH) with these species, is necessary to confirm its classification.These findings highlight the diversity of bacterial genera in the Algerian marine environment, including previously unreported taxa. Therefore, these marine bacteria may serve as a valuable source of potent bioactive metabolites targeting the μ-opioid receptor.

Metabolic profile of bioactive compounds secreted by selected strains

The three Actinobacteria strains, S5T2H1, S7T2H1, and S56T3J31, were selected for their potent inhibitory effects against the test microorganisms and their distinct taxonomic positions. Their crude extracts were analyzed using high-performance liquid chromatography coupled with high-resolution mass spectrometry (HPLC-HRESIMS) to annotate and identify their secreted secondary metabolites.

Compound annotation of the ethyl acetate extract prepared from strain S56T3J31 revealed nine compounds, including two known compounds, three unknown compounds, and five originating from the culture medium itself (Supplementary Fig. S4, Table S6). The medium-derived compounds were detected at retention times of 4.47, 5.20, 6.30, 7.15, and 7.72 min, corresponding to the known isoflavones genistein, genistin, 6″-O-acetyldaidzin, 6″-O-acetylgenistin, and glycitein, respectively. These findings were established based on LC-HRESIMS analysis of the crude extract prepared from the negative control—5294 medium without strain S56T3J31(Supplementary Fig. S9, Table S8). This analysis enabled the detection of the same four compounds at identical retention times, with similar UV–Vis spectra, molecular weights, and molecular formulas. The major natural source of isoflavones is soybean, which was used as an ingredient in the 5294 medium; therefore, this ingredient is the source of the three isoflavone compounds detected in the crude extract prepared from strain S56T3J31.

The two known peaks, **8** and **77**, detected at retention times of 3.82 and 13.11 min, exhibited molecular ion clusters of [M+H] + at m/z 268.0811 and [M+H] + at m/z 507.2336, corresponding to molecular formulas $C_{12}H_{13}NO_6$ and $C_{25}H_{34}N_2O_9$, respectively. A search for similar molecules with these characteristics in natural product databases, such as Antibase and the Dictionary of Natural Products, revealed that compounds 8 and 77 correlate with A58365A and antimycin A, respectively (Fig. 3, Supplementary Fig. S4, Table S6).

The compound A58365A is a fused tetrahydro-indolizine with carboxyl (position 3), hydroxyl (position 8), and ketone (position 5) functional groups, along with a propanoic acid side chain. It was isolated from *Streptomyces chromofuscus* and is primarily known as an angiotensin-converting enzyme (ACE) inhibitor[60]. Antimycin A, on the other hand, belongs to the macrodiolide (bis-lactone) family, characterized by a nine-membered lactone ring. It is produced by *Streptomyces* spp. and functions as a mitochondrial respiratory inhibitor. As the active ingredient in Fintrol®, Antimycin A is a restricted-use piscicide employed in fisheries management to eliminate invasive species and protect native fish populations[61].

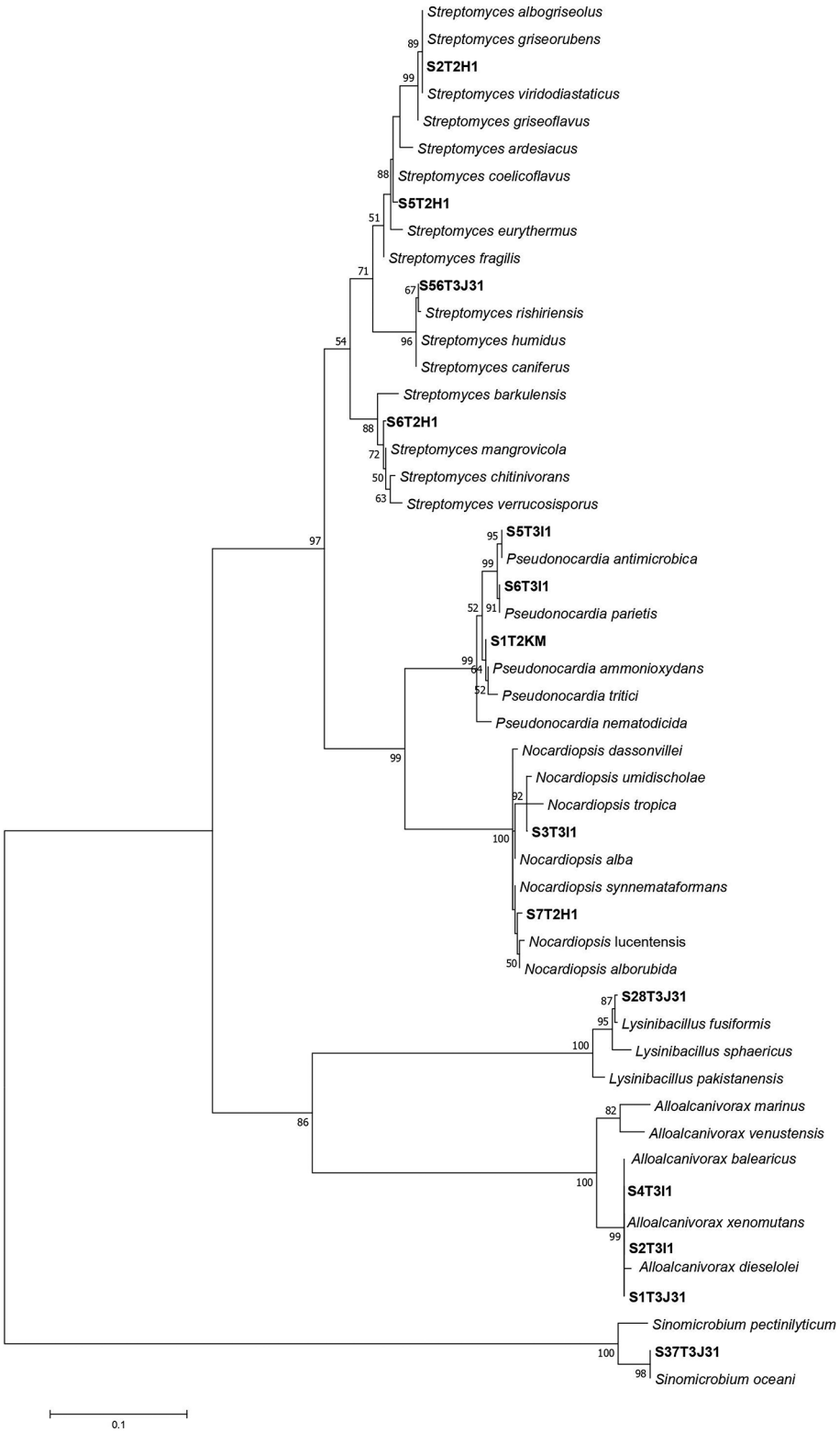

Fig. 2. Molecular phylogenetic analysis by maximum likelihood method, based on almost-complete 16S rRNA gene sequences showing the position and phylogenetic relationship between the some selected strains and the type strains of the closest species. Numbers at the nodes are bootstrap values; expressed as a percentage of 1000 re-samplings (only values 50% are shown).

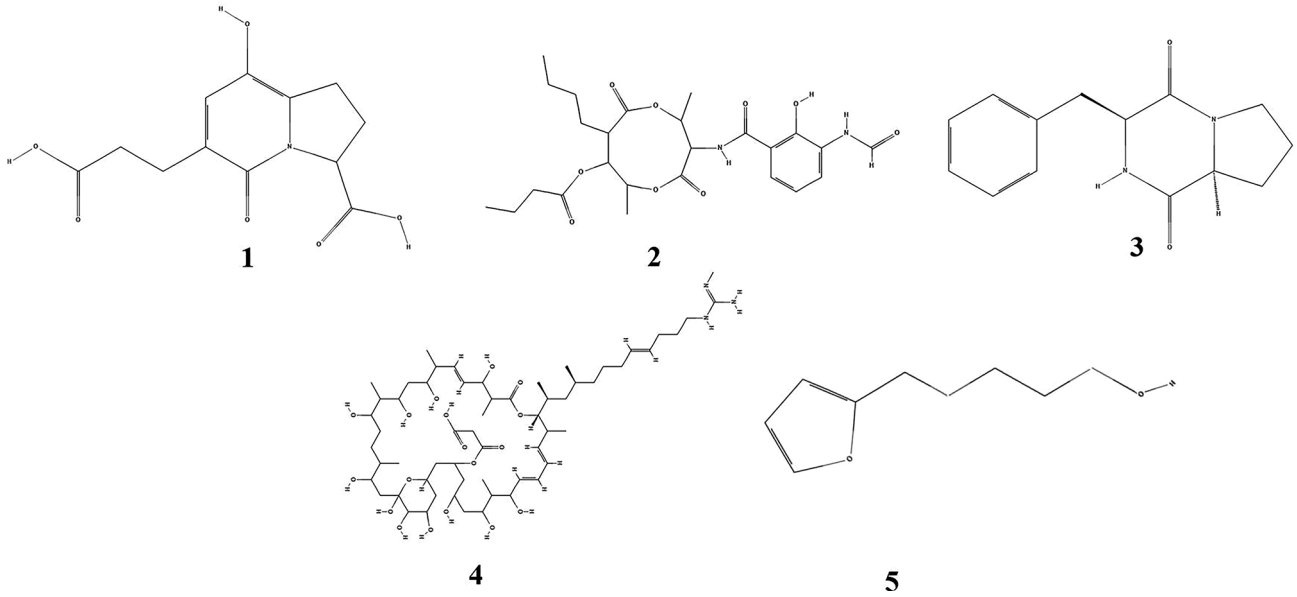

Fig. 3. Structures of compounds identified from crude extract prepared from selected strains: (**1**): A58365A; (**2**): Antimycin A4; (**3**): Cyclo(phenylalanyl-prolyl); (**4**): Niphimycin Ia; (**5**): Berberifuranol.

The molecular formulas of additional peaks found at retention times of 5.25, 6.42, and 12.06 min were established using HPLC–UV-HRESIMS as follows: $C_{30}H_{17}NO_2$, $C_{21}H_{22}O_7$, and $C_{18}H_{20}N_2O_7$ (Supplementary Fig. S4, Table S6). A search across chemical databases revealed no correlated compounds related to actinobacteria or any other microorganisms with similar properties. Therefore, these compounds can presumably be considered unknown.

The LC-HR-ESIMS analysis of the crude extract from strain S5T2H1 revealed several distinct peaks, indicating a complex mixture of metabolites. The compounds identified include both known and potentially novel metabolites, along with two originating from the culture medium at retention times of 5.53 and 7.61 min, corresponding to genistin and glycitein, respectively (Supplementary Fig. S5, Table S7).

Two known compounds, detected at retention times of 4.43 and 11.00 min, were identified as cyclo(phenylalanylprolyl) and the non-ribosomal peptide niphimycin Ia, respectively (Fig. 3, Supplementary Table S7, Fig. S5). Compound Cyclo(phenylalanyl-prolyl), Fig. 3, is a cyclic lipopeptid belonging to the class of diketopiperazines[62]. It is isolated from various microorganisms, including *Actinobacetria*[63,64], *Batrachochytrium dendrobatidis*[65], and *Lactobacillus plantarum*[66]. This compound exhibits a broad spectrum of biological activities, including antimicrobial[64], anti-wax moth larvae (*Galleria mellonella*)[65], and antifungal activities[66]. However, niphimycin Ia is synthesized by several *Streptomyces* species, such as *Streptomyces noursei*. This guanidylpolyol macrolide antibiotic is characterized by its macrolide ring structure, which incorporates guanidyl and polyol groups that contribute to its bioactivity[67].

Furthermore, compounds detected at retention times of 8.36, 8.97, and 11.61 min exhibited molecular ion clusters of [M+H]+ at m/z 356.2908, 381.3036, and 1047.5862, with molecular formulas determined by HPLC–UV-HRESIMS as $C_{19}H_{37}N_3O_3$, $C_{21}H_{39}N_3O_3$, and $C_{53}H_{78}N_{10}O_{12}$, respectively. A search in chemical databases revealed no compounds with similar properties, suggesting that these three compounds may represent novel entities (Supplementary Table S7). These findings align with taxonomic characterization results indicating that strain S5T2H1 may represent a new species within the genus *Streptomyces*, potentially harboring a unique biosynthetic gene cluster responsible for synthesizing these metabolites. This discovery opens the possibility of identifying novel bioactive compounds from this strain[68]. However, confirming the novelty of these metabolites requires purification and structural elucidation using NMR analysis.

LC-HRESIMS analysis of the crude extract secreted by strain S7T2H1 (Supplementary Fig. S6, Table S8), revealed a single active peak with a retention time of approximately 9.17 min. This peak was identified as berberifuranol (Fig. 3) (Supplementary Table S8), exhibiting a molecular ion cluster [M+H]+ at m/z 245.1282, along with UV maxima at 200 nm, 256 nm, and 358 nm (Supplementary Fig. S6). Berberifuranol is a heterocyclic molecule derived from plants, notably isolated from the roots of *Berberis lycium*[69]. This study marks the first reported instance of microbial strain involvement in the biosynthesis of berberifuranol.

In silico study

Conventional opioids act as agonists by interacting with the μ-opioid receptor, providing effective pain relief but often causing severe side effects. Consequently, there is an urgent need to identify new agonists that can deliver analgesic effects without the adverse side effects associated with traditional opioids[70]. A promising approach involves exploring secondary metabolites secreted by marine bacteria as potential sources of novel μ-opioid receptor agonists. In this context, the binding affinity and stability of interactions between the μ-opioid receptor and five distinct marine bacteria-derived compounds—A58365A, Antimycin A4, Cyclo(phenylalanyl-prolyl),

Niphimycin Ia, and Berberifuranol—were compared to each other and to the reference molecule, morphine, using a combination of molecular docking, molecular dynamics simulations and MM/GBSA calculations.

Molecular docking

Molecular docking was performed using the Schrödinger Glide software with XP mode to estimate the binding affinity of five secondary metabolites secreted by marine bacterial strains against the active μ-opioid receptor (5C1M). The results, expressed in kcal/mol, are presented in Table 1:

Based on the docking results (Table 1), the compound A58365A exhibited the strongest binding affinity among the five ligands, with a docking score of − 5.84 kcal/mol, followed closely by Antimycin A4 with a score of − 5.6 kcal/mol. Both ligands displayed slightly weaker affinities compared to the reference molecule, morphine, which exhibited the lowest docking score of − 7.04 kcal/mol, indicating the strongest binding interaction. Lower docking scores reflect stronger predicted interactions between a ligand and the target protein, as less energy is required for the ligand to bind effectively[71]. Therefore, among the tested ligands, compound A58365A is considered to have the highest binding affinity, suggesting it is more likely to form stable interactions through the formation of a stable complex within the receptor's active site of the target protein 5C1M. In contrast, Cyclo(phenylalanyl-prolyl) and Berberifuranol exhibited weaker interactions, with docking scores of − 3.73 and − 3.95 kcal/mol, respectively. However, Niphimycin Ia did not dock successfully, possibly due to its high molecular weight (1142 g/mol) and lack of compatibility with the receptor's binding site (5C1M).

The 3D visualizations were generated to examine the molecular architecture of the binding interactions between the five secondary metabolites and the key residues within the binding cavities of the μ-opioid receptor's active site (5C1M), as illustrated in Fig. 4.

The results in Fig. 4 highlight the critical shared residues, such as Asp147, Met151, Lys233, His297, Val300, and Tyr326, involved in the interactions of all studied ligands within the binding pocket of the target protein 5C1M. These results align with previously published studies, underscoring the importance of these same key residues in target-ligand interactions[72]. Understanding these interactions provides insights into the potential effects of these compounds on the receptor's function. Among the tested compounds, A58365A and Antimycin A4 demonstrated strong interactions with key amino acids within the binding pocket of the μ-opioid receptor (5C1M), as evidenced by their interaction profiles (Fig. 4.1 and 4.2). A58365A primarily engaged through its indolizine ring, forming water-mediated hydrogen bonds with Tyr-148 and Asp-147, hydrophobic contacts with Ile-296, and hydrogen bonding via its propionic acid chain with Lys-269, complemented by a hydrophobic interaction with Val-236 (Fig. 4.1). Similarly, Antimycin A4 exhibited robust binding, primarily through hydrophobic contacts with Leu-291, Asp-147, Val-300, Lys-233, and Ile-296, alongside hydrogen bonds with Cys-217 and Thr-218, and an ionic interaction with Lys-233 (Fig. 4.2). These findings, depicted in Fig. 4, align with the detailed interaction profiles shown in Figs. 5.

Compound A58365A, Fig. 5A, displayed a high interaction strength due to its diverse and dominant water bridges, hydrogen bonds, and hydrophobic contacts, while Antimycin A4's strong binding affinity arose from a combination of substantial water bridges, hydrophobic contacts, and hydrogen bonds (Fig. 5D). In comparison with the reference molecule, (Fig. 5E), both A58365A and Antimycin A4 exhibited interactions comparable to those of morphine, sharing several key amino acids within the active site of 5C1M. These interactions were characterized by a balanced array of hydrogen bonds with Lys-233, hydrophobic interactions with Trp-293, Ile-296, and Tyr-326, and an ionic bond with Asp-147 (Fig. 5E). Similarly, Dumitrascuta et al.[70] reported interactions with key amino acids of 5C1M for structurally related compounds of morphine, such as N-methylmorphinans-6-ones, which engaged hydrophobic residues V236, I296, and V300. Thereby, these findings suggest a potential similarity in the mechanisms of action and binding properties of A58365A and Antimycin A4 with Morphine[73].

Berberifuranol, Fig. 5B, and cyclo(phenylalanyl-prolyl), Fig. 5C, exhibited moderate to low interaction profiles, primarily characterized by water bridges and hydrophobic contacts. Berberifuranol formed fewer hydrogen bonds involving residues such as Val-236 and Tyr-326, slightly reducing its binding strength compared to A58365A. Similarly, cyclo(phenylalanyl-prolyl) demonstrated limited hydrogen bonding with Asp-147 and Val-296, and the absence of ionic bonds further weakened its overall interaction with the receptor.

Molecular dynamic simulation analysis

To investigate the dynamic properties of the docked complexes, Root-Mean-Square Deviation (RMSD) analyses were performed using the Schrödinger Desmond program to evaluate the stability of the μ-opioid receptor (5C1M) in complex with six different ligands, including the reference molecule, over a 100 ns simulation period[71]. Figure 6 presents the RMSD graphs of these complexes during the 100 ns timeframe.

Compounds	Ligands	Docking score (kcal/mol)
1	A58365A	− 5.84
2	Antimycin A4	− 5.6
3	Cyclo(phenylalanyl-prolyl)	− 3.73
4	Niphimycin Ia	Not dock
5	Berberifuranol	− 3.95
6	Morphine	− 7.04

Table 1. Binding energy of docked ligands against the target protein receptor 5C1M.

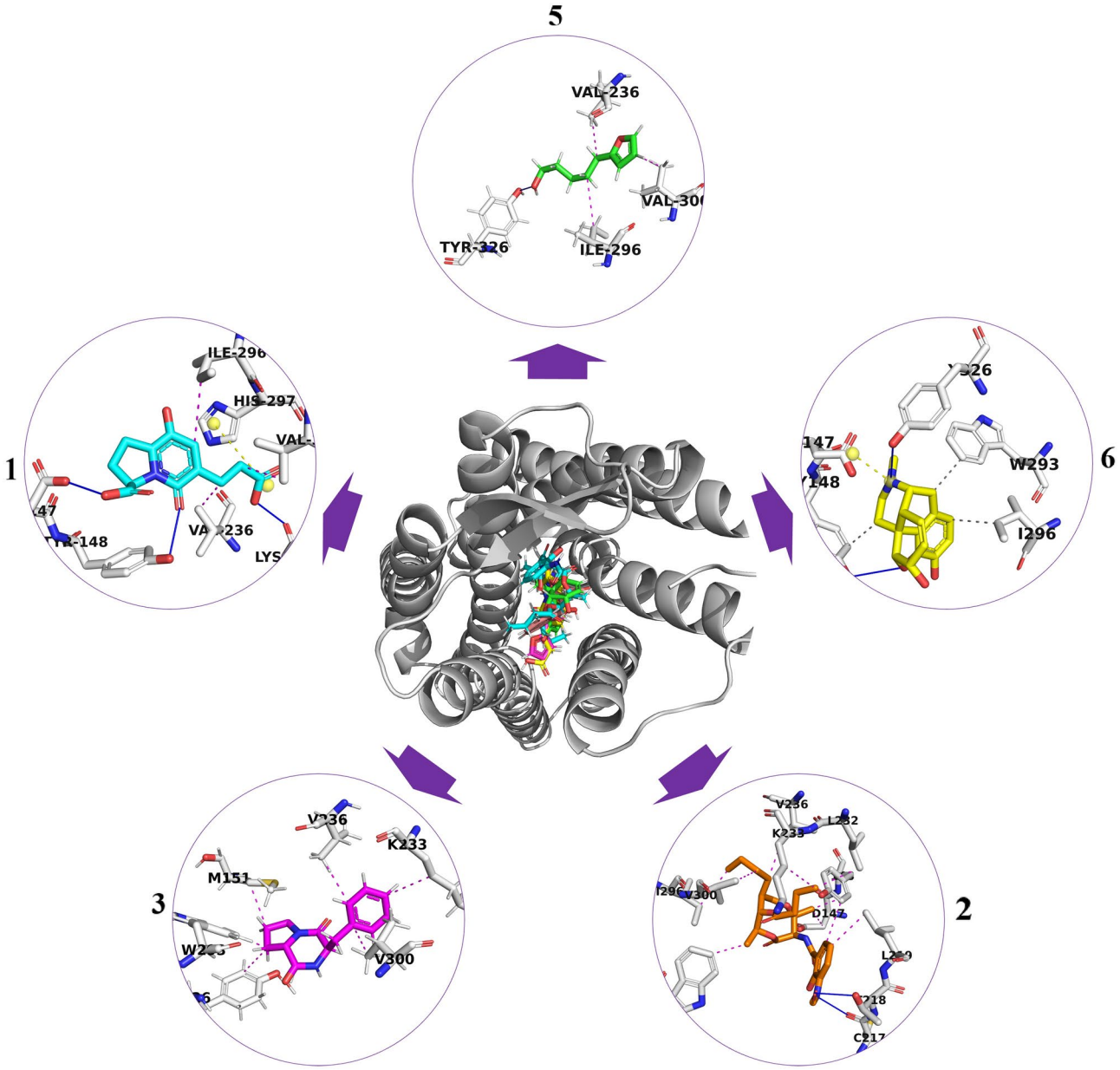

Fig. 4. Docked poses of: **1.** A58365A, **2.** Antimycin A4; **3.** Cyclo(phenylalanyl-prolyl). **5.** Berberifuranol and **6.** Morphine program (Maestro version 14.2.118, Schrödinger Release 2024-3).

The RMSD plot of 5C1M-A58365A (Fig. 6A) shows an initial fluctuation between 20 and 30 ns before reaching a relatively stable conformation. After the equilibration phase, the RMSD remains stable, fluctuating modestly between 3.8 and 4.0 Å. A lower and more stable RMSD indicates minimal fluctuation of the complex. Therefore, the 5C1M-A58365A complex demonstrates greater stability and structural integrity throughout the interaction[74,75]. In contrast, the reference molecule morphine (Fig. 6E) exhibits higher RMSD fluctuations, ranging from 2.5 to 4.7 Å, compared to A58365A. This suggests that the 5C1M-morphine complex undergoes weaker dynamic binding interactions.

Furthermore, both complexes, 5C1M-Cyclo(phenylalanyl-prolyl), Fig. 6C, and 5C1M-Antimycin A4, Fig. 6D, show noticeable fluctuations during the early stages of the simulation, with partial stabilization occurring after ~ 40 ns, eventually exhibiting moderate stability. In contrast, the RMSD values of 5C1M-Berberifuranol complex, Fig. 6B, remain relatively high with significant fluctuations, indicating a less stable complex[76]. The docked complex was used to analyze the Root Mean Square Fluctuation (RMSF) behavior, and a plot was generated incorporating the RMSF, B factor, and interactions to assess the flexibility of individual residues in the ligand–protein complexes. The detailed results are depicted in Fig. 7.

The Root Mean Square Fluctuation (RMSF) analysis evaluates the average positional deviation of residues in the μ-opioid receptor (5C1M) relative to their reference positions throughout the molecular dynamics simulation[77]. For the 5C1M-A58365A complex, RMSF values range from 0.8 to 4.0 Å (Fig. 7A), with the highest

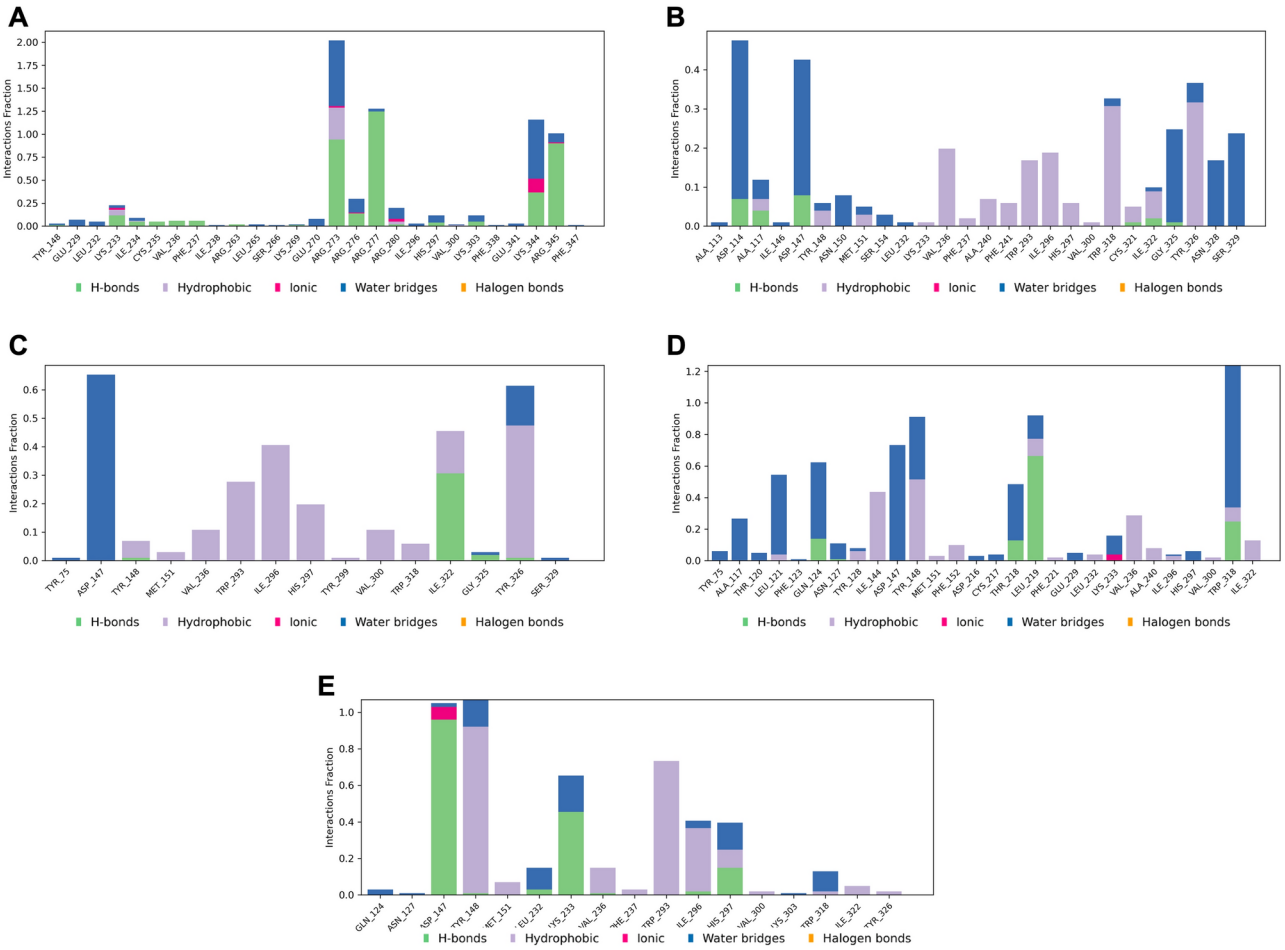

Fig. 5. Protein–ligand interaction profile in complexes: (**A**) 5C1M-A58365A, (**B**) 5C1M -Berberifuranol; (**C**) 5C1M-Cyclo(phenylalanyl-prolyl). (**D**) 5C1M-Antimycin A4 and (**E**) 5C1M-Morphine. Different bar colors represent different types of connections: hydrogen bonds (green), hydrophobic contacts (purple), ionic bonds and water bridges in blue.

fluctuation observed at residue 210, which is located in a non-critical region of the receptor, neither contributing to the active site nor forming direct interactions with A58365A.

In contrast, the RMSF profile for the 5C1M-morphine complex, Fig. 7E, and the four other marine-derived compounds exhibits higher fluctuations, ranging from 0.9 to 6.0 Å. Notably, A58365A was the only compound with RMSF values consistently below 4.0 Å, indicating greater receptor stability upon binding. Since higher RMSF values generally correlate with reduced protein stability and weaker binding interactions, while lower values indicate stronger ligand affinity, these suggest that A58365A provides superior stabilization of the μ-opioid receptor compared to the other tested compounds, including morphine[78].

The atomic flexibility within the 5C1M-A58365A complex was further evaluated using the B-factor curve (pink line). Peaks in B-factor values indicate regions of high mobility, whereas valleys correspond to structurally rigid areas. The RMSF and B-factor values, Fig. 7A, align well in both the A58365A and morphine complexes (Fig. 7E). However, residues 145–155 and 225–235, in both complex (Fig. 7A and E), exhibit notable peaks, suggesting increased structural flexibility in these regions due to ligand binding. Results from RMSD and RMSF analyses indicate that A58365A exhibits strong and stable binding interactions with the target protein 5C1M, compared to morphine. Additionally, A58365A effectively stabilizes the μ-opioid receptor's binding regions while maintaining natural flexibility in non-essential areas. Therefore, these findings highlight A58365A as a promising μ-opioid receptor agonist for further pharmacological investigation.

Figure 8 depicts the ligand characteristics inside the complex, including RMSD, radius of gyration (rGyr), molecular surface area (MolSA), intramolecular hydrogen bonds (intraHB), solvent-accessible surface area (SASA) and polar surface area (PSA), of all the three complexes[76]. These parameters provide valuable insights into various facets of ligand behavior, including structural stability, compactness, surface properties, conformational changes and interactions within the complex, respectively[79].

Considering the results in Fig. 8, among the ligands, A58365A demonstrated the most favorable interaction profile during the 100 ns simulation. This is due to its small fluctuations, observed between 0.1 and 0.4 Å, which remained below 1 Å throughout the entire simulation period with minimal deviation. This indicates stability

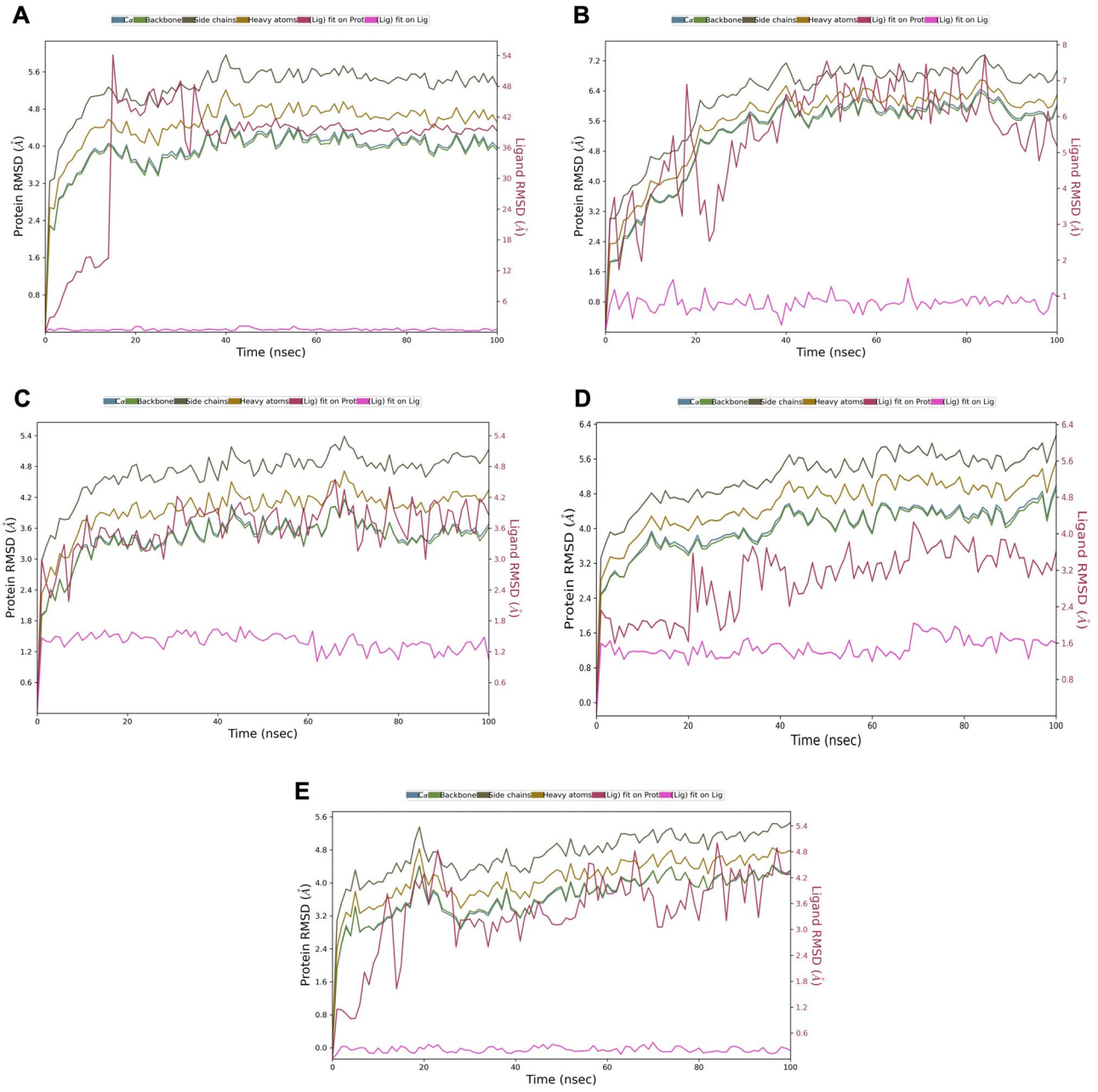

Fig. 6. RMSD plot of μ-opioid receptor target and five marine bacteria-derived compounds as a function of simulation time. (**A**) 5C1M-A58365A, (**B**) 5C1M -Berberifuranol; (**C**) 5C1M-Cyclo(phenylalanyl-prolyl). (**D**) 5C1M-Antimycin A4 and (**E**) 5C1M-Morphine.

and minimal displacement from the initial binding pose, reflecting a strong and reliable interaction between the ligand and the protein[71,76].

In contrast, the other four ligands exhibited significant fluctuations in RMSD, ranging between 0.8 and 1.8 Å, indicating relatively less stable binding interactions with the protein. However, regarding the reference compound, morphine, its RMSD values remained consistently lower (~ 0.15–0.35 Å), similar to A58365A, with relatively small fluctuations. This suggests that the ligand maintains a stable position throughout the simulation[78]. Additionally, A58365A exhibits a stable radius of gyration (rGyr), fluctuating around 3.3–3.5 Å, indicating a relatively compact conformation during the simulation. It also maintains balanced solvent exposure (SASA), a stable molecular surface area (MolSA), and consistent polar interactions (PSA). These attributes collectively indicate strong and stable binding to 5C1M.

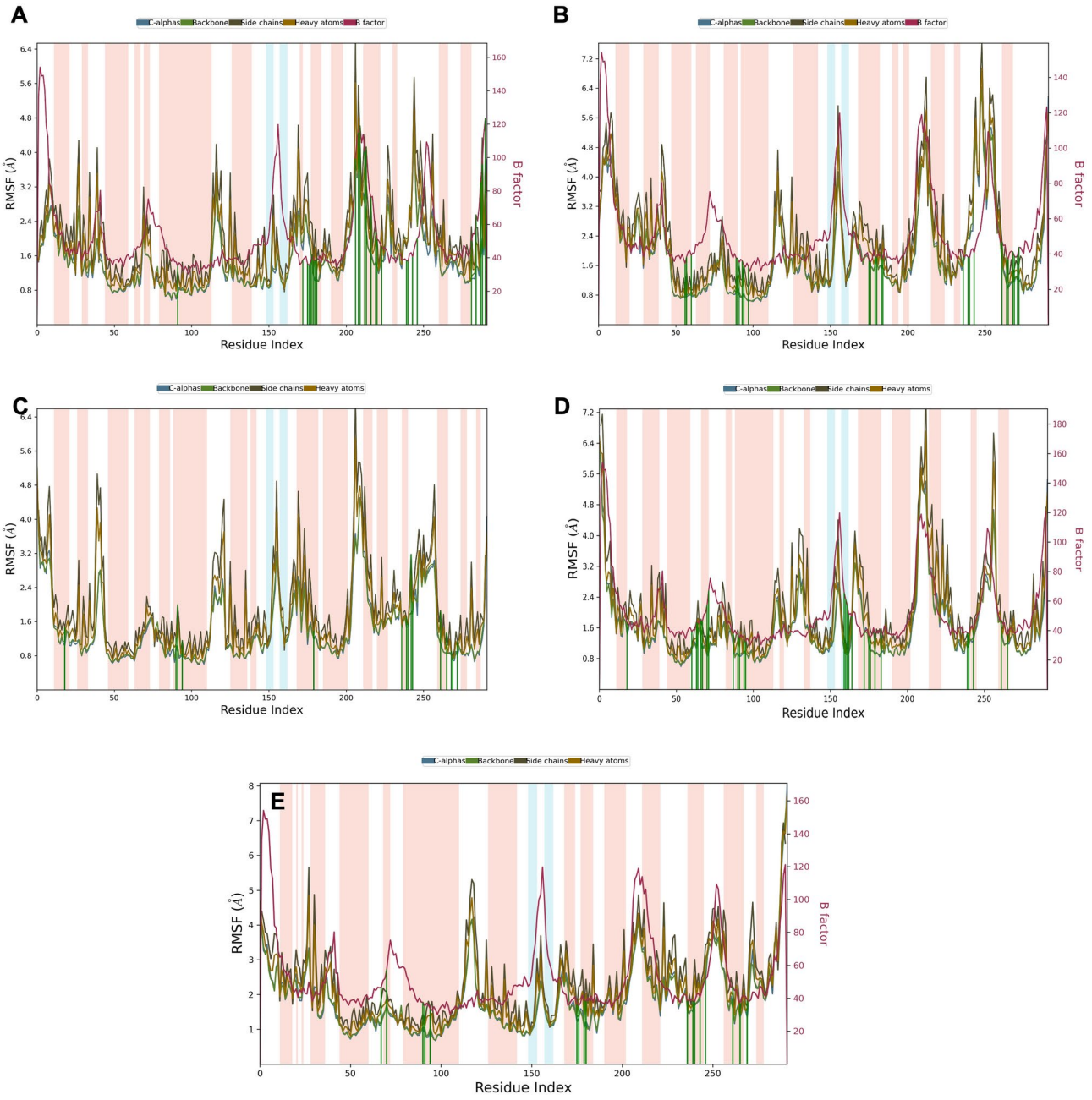

Fig. 7. MD simulation protein–ligand interaction root-mean-square fluctuation (RMSF) profile. (**A**) 5C1M-A58365A, (**B**) 5C1M -Berberifuranol; (**C**) 5C1M-Cyclo(phenylalanyl-prolyl). (**D**) 5C1M-Antimycin A4 and (**E**) 5C1M-Morphine.

MM/GBSA binding free energy calculations

The binding free energy of the complexes was computed using the Maestro prime module's MM/GBSA approach, which is generally recognized for its efficacy in measuring ligand-binding affinities within protein systems[80], the results are shown in Table 2.

Based on the MM/GBSA profiles of the MD simulations for the five complexes, the 5C1M-A58365A complex exhibits comparable interaction parameters to the reference morphine, indicating a well-balanced equilibrium between the different interaction forces[30]. This balance is reflected in its stable binding free energy (ΔG bind = – 46.66 kcal/mol), which is close to that of the reference complex 5C1M-morphine (– 53.55 kcal/mol). The ΔG bind Coulomb (– 6.24 kcal/mol) is also similar to that of morphine (– 6.64 kcal/mol), suggesting comparable electrostatic contributions to binding[81,82].

Additionally, the 5C1M-A58365A complex demonstrates a balanced binding profile in other aspects. Its covalent binding energy (1.75 kcal/mol) is slightly higher than that of morphine (1.26 kcal/mol), ensuring stability without excessive rigidity. Furthermore, its van der Waals contribution (– 38.53 kcal/mol) is well-

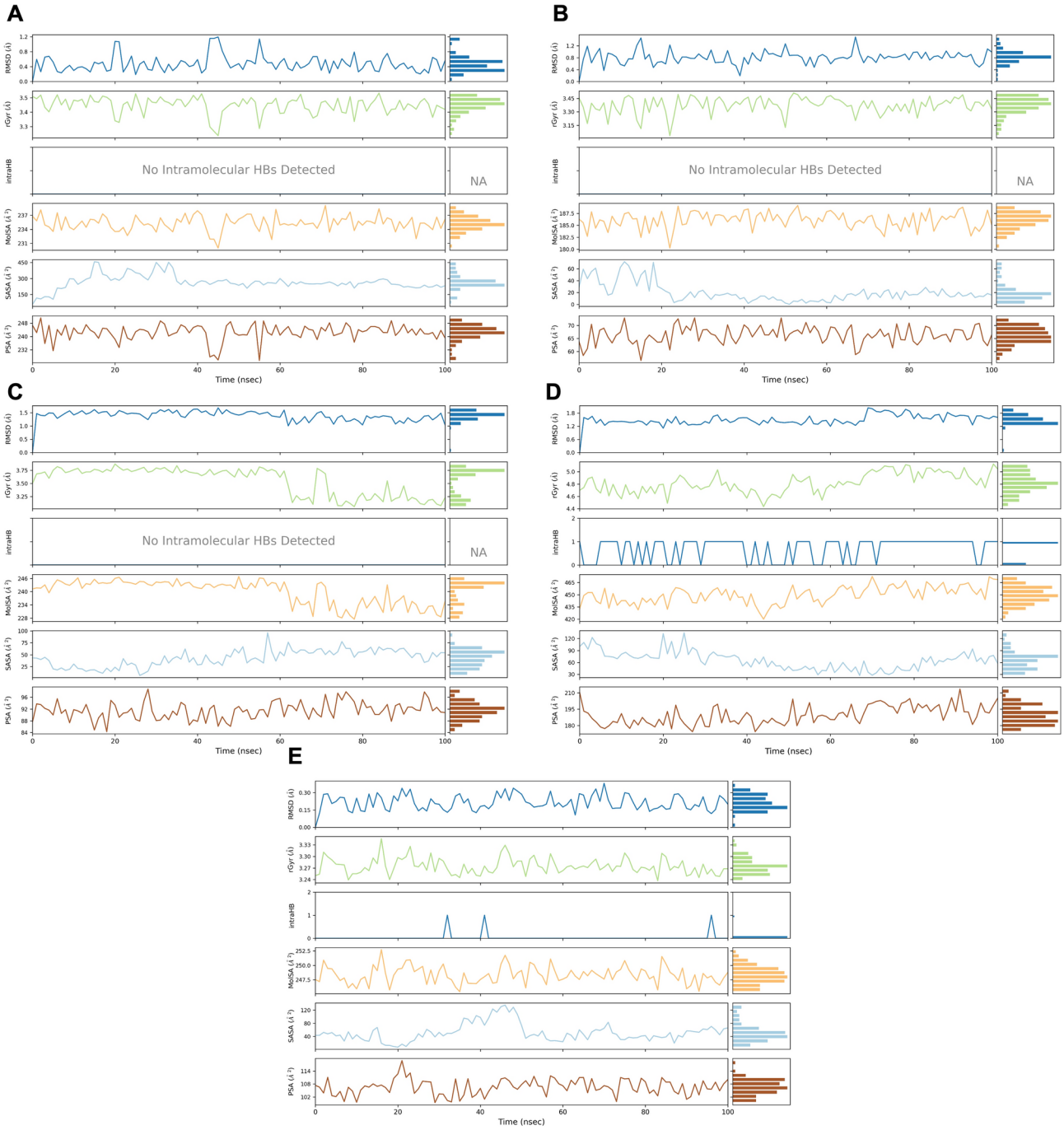

Fig. 8. Ligand properties for: (**A**) A58365A, (**B**) Berberifuranol, (**C**) Cyclo(phenylalanyl-prolyl), (**D**) Antimycin A4 and (**E**) Morphine, with 5C1M protein, such as RMSD, the radius of gyration (rGyr), intramolecular hydrogen bonds (intraHB), molecular surface area (MolSA), solvent accessible surface area (SASA), polar surface area (PSA) on interacting with protein during MD simulation.

balanced, providing optimal hydrophobic interactions without being excessively strong or weak[22]. These results confirm the findings from molecular docking and molecular dynamics simulations, further suggesting that compound A58365A exhibits strong and stable interactions with the target 5C1M. This indicates that A58365A could potentially serve as a promising candidate for targeting 5C1M with favorable binding properties[68,71].

Conclusion

This study highlights the potential of marine-derived bacterial compounds as promising alternatives to conventional opioid drugs. By investigating bacterial strains isolated from marine sediments along the Bejaia coastline (Algeria), 45 marine bacteria were obtained using six different culture media, with SCA proving to be the most effective. Molecular identification, based on 16S rRNA gene sequencing, revealed that 18 strains,

Complexes	ΔG bind (kcal/mol)	ΔG bind Coulomb (kcal/mol)	ΔG bind covalent (kcal/mol)	ΔG bind H bond (kcal/mol)	ΔG binding SolvGB (kcal/mol)	ΔG bind Vander (kcal/mol)
5C1M-A58365A	− 46.66	− 6.24	1.75	− 0.23	15.94	− 38.53
5C1M-berberifuranol	− 37.77	− 7.97	1.18	− 0.43	14.61	− 27.83
5C1M-cyclo(phenylalanyl-prolyl)	− 25.80	− 276.80	1.09	− 4.80	269.56	− 12.10
5C1M-Antimycin	− 55.13	− 70.02	0.99	− 0.89	90.41	− 56.21
5C1M-Morphie	− 53.55	− 6.64	1.26	− 1.38	10.80	− 34.97

Table 2. MM/GBSA profiles of the MD simulated complexes.

selected for their potent antimicrobial activity against various pathogenic microorganisms, belonged to six genera: *Streptomyces, Nocardiopsis, Alloalcanivorax, Pseudonocardia, Sinomicrobium*, and *Lysinibacillus*. LC-HRESIMS analysis of secondary metabolites secreted by three selected strains (*S5T2H1, S56T3J31,* and *S7T2H1*) identified five known compounds—A58365A, antimycin A, cyclo(phenylalanyl-prolyl), niphimycin Ia, and berberifuranol—along with several unknown metabolites. Molecular docking and molecular dynamics simulations demonstrated that A58365A exhibited strong and stable interactions with the μ-opioid receptor (5C1M), comparable to morphine. These findings suggest that marine bacteria represent an untapped reservoir of opioid-like bioactive molecules with significant therapeutic potential. Further structural elucidation, in vitro and in vivo studies, and pharmacokinetic assessments are necessary to validate their efficacy and safety as novel analgesics. This research underscores the importance of marine microbial biodiversity in drug discovery and paves the way for developing safer opioid alternatives with reduced side effects.

Data availability

The datasets used and/or analysed during the current study available from the corresponding author on reasonable request.

Received: 11 June 2024; Accepted: 27 March 2025
Published online: 17 May 2025

References

1. Mazzeo, F., Meccariello, R. & Guatteo, E. Molecular and epigenetic aspects of opioid receptors in drug addiction and pain management in sport. *Int. J. Mol. Sci.* **24**(9), 7831. https://doi.org/10.3390/ijms24097831 (2023).
2. Fürst, S. & Hosztafi, S. The chemical and pharmacological importance of morphine analogues. *Acta Physiol. Hung.* **95**(1), 3–44. https://doi.org/10.1556/APhysiol.95.2008.1.1 (2008).
3. Benyhe, S. Morphine: New aspects in the study of an ancient compound. *Life Sci.* **55**(13), 969–979. https://doi.org/10.1016/0024-3205(94)00631-8 (1994).
4. Noha, S. M., Schmidhammer, H. & Spetea, M. Molecular docking, molecular dynamics, and structure-activity relationship explorations of 14-oxygenated N-methylmorphinan-6-ones as potent μ-opioid receptor agonists. *ACS Chem. Neurosci.* **8**(6), 1327–1337. https://doi.org/10.1021/acschemneuro.6b00460 (2017).
5. Meissner, K. et al. Morphine and hydromorphone effects, side effects, and variability: A crossover study in human volunteers. *Anesthesiology* **139**(1), 16–34. https://doi.org/10.1097/ALN.0000000000004567 (2023).
6. Ngamcharungchit, C., Chaimusik, N., Panbangred, W., Euanorasetr, J. & Intra, B. Bioactive metabolites from terrestrial and marine actinomycetes. *Molecules* **28**(15), 5915. https://doi.org/10.3390/molecules28155915 (2023).
7. Damiescu, R. et al. Aniquinazoline B, a fungal natural product, activates the μ-opioid receptor. *ChemMedChem* **19**(19), e202400213. https://doi.org/10.1002/cmdc.202400213 (2024).
8. Messaoudi, O. et al. Characterization of silver carbonate nanoparticles biosynthesized using marine actinobacteria and exploring of their antimicrobial and antibiofilm activity. *Mar. Drugs.* **21**(10), 536. https://doi.org/10.3390/md21100536 (2023).
9. Feknous, N., Branes, Z., Rouabhia, K., Batisson, I. & Amblard, C. Isolation characterization and growth of locally isolated hydrocarbonoclastic marine bacteria (eastern Algerian coast). *Environ. Monit. Assess.* **189**(2), 49. https://doi.org/10.1007/s10661-016-5758-5 (2017).
10. Quinn, G. A. & Dyson, P. J. Going to extremes: progress in exploring new environments for novel antibiotics. *npj Antimicrob. Resist.* **2**, 8. https://doi.org/10.1038/s44259-024-00025- (2024).
11. Schumacher, B. A. Methods for the determination of total organic carbon (TOC) in soils and sediments. 1–23 (US Environmental Protection Agency, Office of Research and Development, Ecological Risk Assessment Support Center, 2003).
12. Jensen, P. R., Gontang, E., Mafnas, C., Mincer, T. J. & Fenical, W. Culturable marine actinomycete diversity from tropical Pacific Ocean sediments. *Environ. Microbiol.* **7**(7), 1039–1048. https://doi.org/10.1111/j.1462-2920.2005.00785.x (2005).
13. Messaoudi, O., Wink, J., & Bendahou, M. Diversity of Actinobacteria Isolated from Date Palms Rhizosphere and Saline Environments: Isolation, Identification and Biological Activity Evaluation. *Microorganisms.* **8**, 1853. https://doi.org/10.3390/microorganisms8121853 (2020).
14. Mincer, T. J., Jensen, P. R., Kauffman, C. A. & Fenical, W. Widespread and persistent populations of a major new marine actinomycete taxon in ocean sediments. *Appl. Environ. Microbiol.* **68**(10), 5005–5011. https://doi.org/10.1128/AEM.68.10.5005-5011 (2002).
15. Magarvey, N. A., Keller, J. M., Bernan, V., Dworkin, M. & Sherman, D. H. Isolation and characterization of novel marine-derived actinomycete taxa rich in bioactive metabolites. *Appl. Environ. Microbiol.* **70**(12), 7520–7529. https://doi.org/10.1128/AEM.70.12.7520-7529.2004 (2004).
16. Matan, N. & Matan, N. Antifungal activities of anise oil, lime oil, and tangerine oil against molds on rubberwood (*Hevea brasiliensis*). *Int. Biodeterior. Biodegrad.* **62**, 75–78. https://doi.org/10.1016/j.ibiod.2007.07.014 (2008).
17. Yahla, S. et al. Exploring Teucrium Aureo-Candidum Essential Oil as a Promising Alternative to Triclosan for Targeting Enoyl-Acyl Carrier Protein Reductase: Chemical Composition, Antibacterial Activity, and Molecular Docking Study. *Chem Biodivers.* **22**, e202401945. https://doi.org/10.1002/cbdv.202401945 (2024).

18. Patel, J. J. & Brown, M. E. Interactions of azotobacter with rhizosphere and root-surface microflora. *Plant Soil* **31**, 273–281. https://doi.org/10.1007/BF01373570 (1969).
19. Messaoudi, O. Contribution à la Caractérisation des Souches D'Actinomycètes Productrice des Métabolites Antibactériennes Isolée de la Sebkha de Kendasa (Bechar). Master's Thesis, Université of Tlemcen, Tlemcen, Algeria, (2013).
20. Lampert, Y. et al. Phylogenetic diversity of bacteria associated with the mucus of Red Sea corals. *FEMS Microbiol. Ecol.* **64**(2), 187–198. https://doi.org/10.1111/j.1574-6941.2008.00458.x (2008) (**Epub 2008 Mar 18**).
21. Shirling, E. B. & Gottlieb, D. Methods for characterization of Streptomyces species. *Int. Syst. Bacteriol.* **16**, 313–340 (1966).
22. Genheden, S. & Ryde, U. The MM/PBSA and MM/GBSA methods to estimate ligand-binding affinities. *Expert Opin. Drug Discov.* **10**(5), 449–461. https://doi.org/10.1517/17460441.2015.1032936 (2015).
23. Glättli, A., Daura, X. & van Gunsteren, W. F. Derivation of an improved simple point charge model for liquid water: SPC/A and SPC/L. *J. Chem. Phys.* **116**(22), 9811–9828 (2002).
24. Jorgensen, W. L., Maxwell, D. S. & Tirado-Rives, J. Development and testing of the OPLS all-atom force field on conformational energetics and properties of organic liquids. *J. Am. Chem. Soc.* **118**(45), 11225–11236 (1996).
25. Jorgensen, W. L. & Tirado-Rives, J. The OPLS [optimized potentials for liquid simulations] potential functions for proteins, energy minimizations for crystals of cyclic peptides and crambin. *J. Am. Chem. Soc.* **110**(6), 1657–1666 (1988).
26. Bowers, K. J. et al. Scalable algorithms for molecular dynamics simulations on commodity clusters. In *Proceedings of the ACM/IEEE Conference on Supercomputing (SC06), Tampa, Florida, 2006, November 11–17* (2006).
27. Desmond Molecular Dynamics System, D. E. Shaw Research, 2024. Maestro-Desmond Interoperability Tools, Schrödinger, (2024).
28. Mark, P. & Nilsson, L. Structure and dynamics of the TIP3P, SPC, and SPC/E water models at 298 K. *J. Phys. Chem. A* **105**(43), 9954–9960 (2001).
29. Shivakumar, D. et al. Prediction of absolute solvation free energies using molecular dynamics free energy perturbation and the OPLS force field. *J. Chem. Theory Comput.* 6, 1509–1519. https://doi.org/10.1021/ct900587b (2010).
30. Patel, C. N., Mall, R. & Bensmail, H. AI-driven drug repurposing and binding pose meta dynamics identifies novel targets for monkeypox virus. *J. Infect. Public Health* **16**(5), 799–807 (2023).
31. Ghare, P. M. & Kumbhar, A. P. Study on physico chemical parameters of soil sample. *Iarjset* **8**(9), 171–187. https://doi.org/10.17148/iarjset.2021.8930 (2021).
32. Okafor, U. C. Evaluation of the impact of crude oil contamination on soil's physicochemical characteristics, micro-flora and crop yield. *Trop. Aquat. Soil Pollut.* **3**(1), 24–35. https://doi.org/10.53623/tasp.v3i1.132 (2023).
33. Zhou, Z., Wang, C. & Luo, Y. Meta-analysis of the impacts of global change factors on soil microbial diversity and functionality. *Nat. Commun.* https://doi.org/10.1038/s41467-020-16881-7 (2020).
34. Sudha, S. & Masilamani, S. M. Characterization of cytotoxic compound from marine sediment derived actinomycete Streptomyces avidinii strain SU4. *Asian Pac. J. Trop. Biomed.* **2**(10), 770–773. https://doi.org/10.1016/S2221-1691(12)60227-5 (2012).
35. Priyanka, S. et al. Characterisation and identification of antibacterial compound from marine actinobacteria: In vitro and in silico analysis. *J. Infect. Public Health.* **12**(1), 83–89. https://doi.org/10.1016/j.jiph.2018.09.005 (2019).
36. Ramasamy, V., Durairaj, T., Alagappan, C. & Sudalaimuthu, R. S. S. Cultivation techniques of rare actinobacteria. In *Methods in Actinobacteriology. Springer Protocols Handbooks* (ed Dharumadurai, D.) https://doi.org/10.1007/978-1-0716-1728-1_25 (Humana, 2022).
37. Yu, J. et al. Isolation and characterization of actinobacteria from Yalujiang coastal wetland, North China. *Asian Pac. J. Trop. Biomed.* **5**(7), 555–560. https://doi.org/10.1016/j.apjtb.2015.04.007 (2015).
38. Huang, Z. et al. A simple culture method enhances the recovery of culturable actinobacteria from coastal sediments. *Front. Microbiol.* **14**(12), 675048. https://doi.org/10.3389/fmicb.2021.675048 (2021).
39. Messaoudi, O., Steinmann, E., Praditya, D., Bendahou, M. & Wink, J. Taxonomic characterization, antiviral activity and induction of three new kenalactams in *Nocardiopsis* sp. CG3. *Curr. Microbiol.* **79**(9), 284. https://doi.org/10.1007/s00284-022-02954-x (2022).
40. Crawford, D. L., Lynch, J. M., Whipps, J. M. & Ousley, M. A. Isolation and characterization of actinomycete antagonists of a fungal root pathogen. *Appl. Environ. Microbiol.* **59**(11), 3899–3905. https://doi.org/10.1128/aem.59.11.3899-3905.1993 (1993).
41. Boudemagh, A. et al. Isolation and molecular identification of actinomycete microflora, of some saharian soils of south east Algeria (Biskra, EL-Oued and Ourgla) study of antifungal activity of isolated strains. *Journal de Mycologie Médicale* **15**(1), 39–44 (2005).
42. Messaoudi, O. Isolement et Caractérisation de Nouvelles Molécules Bioactives à Partir D'Actinomycètes Isolées du sol Algérien. Ph.D. Thesis, Université de Tlemcen, Tlemcen, Algeria, 2020.
43. Srinivasan, R., Kannappan, A., Shi, C. & Lin, X. Marine bacterial secondary metabolites: A treasure house for structurally unique and effective antimicrobial compounds. *Mar. Drugs.* **19**(10), 530. https://doi.org/10.3390/md19100530 (2021).
44. Debbab, A., Aly, A. H., Lin, W. H. & Proksch, P. Bioactive compounds from marine bacteria and fungi. *Microb. Biotechnol.* **3**(5), 544–563. https://doi.org/10.1111/j.1751-7915.2010.00179.x (2010).
45. Bharathi, D. & Lee, J. Recent advances in marine-derived compounds as potent antibacterial and antifungal agents: A comprehensive review. *Mar. Drugs.* **22**(8), 348. https://doi.org/10.3390/md22080348 (2024).
46. Johnson, T. A. et al. Identification of the first marine-derived opioid receptor "balanced" agonist with a signaling profile that resembles the endorphins. *ACS Chem. Neurosci.* **8**(3), 473–485. https://doi.org/10.1021/acschemneuro.6b00167 (2017).
47. Chakraborty, S. et al. A novel mitragynine analog with low-efficacy mu opioid receptor agonism displays antinociception with attenuated adverse effects. *J. Med. Chem.* **64**(18), 13873–13892 (2021).
48. Fadhilah, Q. G., Santoso, I., Maryanto, A. E., Abdullah, S. & Yasman, Y. Evaluation of the antifungal activity of marine actinomycetes isolates against the phytopathogenic fungi Colletotrichum siamense KA: A preliminary study for new antifungal compound discovery. *Pharmacia* **68**(4), 837–843 (2021).
49. Sangkanu, S., Rukachaisirikul, V., Suriyachadkun, C. & Phongpaichit, S. Antifungal activity of marine-derived actinomycetes against Talaromyces marneffei. *J. Appl. Microbiol.* **130**(5), 1508–1522. https://doi.org/10.1111/jam.14877 (2021).
50. Thawabteh, A. M. et al. Antifungal and antibacterial activities of isolated marine compounds. *Toxins* **15**(2), 93. https://doi.org/10.3390/toxins15020093 (2023).
51. Ravikumar, S., Thajuddin, N., Suganthi, P., Inbaneson, S. J. & Vinodkumar, T. Bioactive potential of seagrass bacteria against human bacterial pathogens. *J. Environ. Biol.* **31**(3), 387–389 (2010).
52. Djinni, I., Defant, A., Kecha, M. & Mancini, I. Actinobacteria derived from algerian ecosystems as a prominent source of antimicrobial molecules. *Antibiotics* **8**(4), 172. https://doi.org/10.3390/antibiotics8040172 (2019).
53. Lai, Q., Wang, J., Gu, L., Zheng, T. & Shao, Z. *Alcanivorax marinus* sp. nov., isolated from deep-sea water. *Int. J. Syst. Evol. Microbiol.* **63**(Pt 12), 4428–4432. https://doi.org/10.1099/ijs.0.049957-0 (2013).
54. Xu, Y. et al. *Sinomicrobium oceani* gen. nov., sp. nov., a member of the family Flavobacteriaceae isolated from marine sediment. *Int. J. Syst. Evol. Microbiol.* **63**(Pt 3), 1045–1050. https://doi.org/10.1099/ijs.0.041889-0 (2013).
55. Oliveira, M. M. et al. Biofilms of Pseudomonas and Lysinibacillus marine strains on high-density polyethylene. *Microb. Ecol.* **81**(4), 833–846. https://doi.org/10.1007/s00248-020-01666-8 (2021).
56. Cherian, T. et al. Green chemistry based gold nanoparticles synthesis using the marine bacterium *Lysinibacillus odysseyi* PBCW2 and their multitudinous activities. *Nanomaterials* **12**(17), 2940. https://doi.org/10.3390/nano12172940 (2022).
57. Jung, M. Y. et al. Description of *Lysinibacillus sinduriensis* sp. nov., and transfer of *Bacillus massiliensis* and *Bacillus odysseyi* to the genus *Lysinibacillus* as *Lysinibacillus massiliensis* comb. nov. and *Lysinibacillus odysseyi* comb. nov. with emended description of the genus *Lysinibacillus*. *Int. J. Syst. Evol. Microbiol.* **62**(Pt 10), 2347–2355. https://doi.org/10.1099/ijs.0.033837-0 (2012).

58. Kyoung Kwon, K., Hye, Oh. J., Yang, S. H., Seo, H. S. & Lee, J. H. *Alcanivorax gelatiniphagus* sp. nov., a marine bacterium isolated from tidal flat sediments enriched with crude oil. *Int. J. Syst. Evol. Microbiol.* **65**(7), 2204–2208. https://doi.org/10.1099/ijs.0.000244 (2015).
59. Kim, M., Oh, H. S., Park, S. C. & Chun, J. Towards a taxonomic coherence between average nucleotide identity and 16S rRNA gene sequence similarity for species demarcation of prokaryotes. *Int. J. Syst. Evol. Microbiol.* **64**, 346–351. https://doi.org/10.1099/ijs.0.059774-0 (2014).
60. Hunt, A. H. et al. Structure elucidation of A58365A and A58365B, angiotensin converting enzyme inhibitors produced by *Streptomyces chromofuscus*. *J. Antibiot.* **41**(6), 771–779. https://doi.org/10.7164/antibiotics.41.771 (1988).
61. Ma, X. et al. Mitochondrial electron transport chain complex III is required for antimycin A to inhibit autophagy. *Chem. Biol.* **18**(11), 1474–1481. https://doi.org/10.1016/j.chembiol.2011.08.009 (2011).
62. Belal, A., Gouda, A. M., Ahmed, A. S. & Abdel Gawad, N. M. Synthesis of novel indolizine, diazepinoindolizine and Pyrimidoindolizine derivatives as potent and selective anticancer agents. *Res. Chem. Intermed.* **41**, 9687–9701 (2015).
63. Gautschi, M. et al. Chemical characterization of diketopiperazines in beer. *J. Agric. Food Chem.* **45**(8), 3183–3189 (1997).
64. Kannabiran, K. Bioactivity-guided extraction and identification of antibacterial compound from marine actinomycetes strains isolated from costal soil samples of Rameswaram and Dhanushkodi, Tamil Nadu, India. *Asian J. Pharm.* **10**(04) (2016).
65. Starr, A. M., Zabet-Moghaddam, M. & San, F. M. Identification of a novel secreted metabolite cyclo(phenylalanyl-prolyl) from Batrachochytrium dendrobatidis and its effect on Galleria mellonella. *BMC Microbiol.* **22**(1), 293. https://doi.org/10.1186/s12866-022-02680-1 (2022).
66. Ström, K., Sjögren, J., Broberg, A. & Schnürer, J. Lactobacillus plantarum MiLAB 393 produces the antifungal cyclic dipeptides cyclo(L-Phe-L-Pro) and cyclo(L-Phe-trans-4-OH-L-Pro) and 3-phenyllactic acid. *Appl. Environ. Microbiol.* **68**(9), 4322–4327. https://doi.org/10.1128/AEM.68.9.4322-4327.2002 (2002).
67. Chen, Y. et al. Discovery of niphimycin C from *Streptomyces yongxingensis* sp. nov. as a promising agrochemical fungicide for controlling banana fusarium wilt by destroying the mitochondrial structure and function. *J. Agric. Food Chem.* **70**(40), 12784–12795. https://doi.org/10.1021/acs.jafc.2c02810 (2022).
68. Messaoudi, O., Sudarman, E., Patel, C., Bendahou, M. & Wink, J. Metabolic profile, biotransformation, docking studies and molecular dynamics simulations of bioactive compounds secreted by CG3 strain. *Antibiotics* **11**(5), 657. https://doi.org/10.3390/antibiotics11050657 (2022).
69. Ali, M. & Sharma, S. K. Heterocyclic constituents from Berberis lycium roots. *Ind. J. Hetero. Chem.* **6**, 127–130 (1996).
70. Dumitrascuta, M. et al. Synthesis, pharmacology, and molecular docking studies on 6-desoxo-N-methylmorphinans as potent μ-opioid receptor agonists. *J. Med. Chem.* **60**(22), 9407–9412. https://doi.org/10.1021/acs.jmedchem.7b01363 (2017).
71. Bouzidi, A. et al. Phytochemical analysis, biological activities of methanolic extracts and an isolated flavonoid from Tunisian *Limoniastrum monopetalum* (L.) Boiss: An in vitro and in silico investigations. *Sci. Rep.* **14**(1), 3281. https://doi.org/10.1038/s41598-024-53821-7.10.1038/s41598-023-46457-6 (2024).
72. Huang, W. et al. Structural insights into μ-opioid receptor activation. *Nature* **524**(7565), 315–321. https://doi.org/10.1038/nature14886 (2015) (**Epub 2015 Aug 5. Erratum in: Nature. 2020;584(7820):E16. doi: 10.1038/s41586-020-2542-z**).
73. Dumitrascuta, M. et al. N-phenethyl substitution in 14-methoxy-N-methylmorphinan-6-ones turns selective μ OPIOID receptor ligands into dual μ/Δ opioid receptor agonists. *Sci. Rep.* **10**(1), 5653. https://doi.org/10.1038/s41598-020-62530-w (2020).
74. Hassan, A. M. et al. Evaluating the binding potential and stability of drug-like compounds with the monkeypox virus VP39 protein using molecular dynamics simulations and free energy analysis. *Pharmaceuticals.* **17**(12), 1617. https://doi.org/10.3390/ph17121617 (2024).
75. Moschovou, K. et al. Exploring the binding effects of natural products and antihypertensive drugs on SARS-CoV-2: An in silico investigation of main protease and spike protein. *Int. J. Mol. Sci.* **24**(21), 15894. https://doi.org/10.3390/ijms242115894 (2023).
76. Tahira, S. et al. N-aroyl-N′-(1-Naphthyl)-N′′-aryl guanidines as a new entry to urease inhibitors: Synthesis, kinetic mechanism, molecular docking and MD simulation studies. *ChemistrySelect* **8**(15), e202300339. https://doi.org/10.1002/slct.202300339 (2023).
77. Messaoudi, O. et al. Berries anthocyanins as potential SARS-CoV–2 inhibitors targeting the viral attachment and replication; molecular docking simulation. *Egypt. J. Pet.* **30**(1), 33–43 (2021).
78. Adebayo-Gege, G. et al. Molecular modeling of the interactions of Curcuma longa compounds with VEGFR towards colorectal cancer drug development. *Inform. Med. Unlocked* **43**, 101376 (2023).
79. Kaur, G., Bansal, M., Rehman, H. M., Kaur, M. & Kaur, A. Synthesis and studies of new purines/pyrimidine derivatives as multi-targeted agents involving various receptor sites in the immune system. *Mol. Divers.* **28**(1), 97–110. https://doi.org/10.1007/s11030-023-10616-8 (2024).
80. Defant, A., Innocenti, N. & Mancini, I. 3a-(4-Chlorophenyl)-1-methyl-3a,4-dihydroimidazo[1,5-a]quinazolin-5(3H)-one: Synthesis and in silico evaluation as a ligand in the μ-opioid receptor. *Molbank* **2023**, M1622. https://doi.org/10.3390/M1622 (2023).
81. Zhou, F., Yao, H., Ma, Z. & Hu, X. Investigating small molecule compounds targeting psoriasis based on cMAP database and molecular dynamics simulation. *Skin Res. Technol.* **29**(4), e13301. https://doi.org/10.1111/srt.13301 (2023).
82. Podlewska, S., Bugno, R., Kudla, L., Bojarski, A. J. & Przewlocki, R. Molecular modeling of μ opioid receptor ligands with various functional properties: PZM21, SR-17018, morphine, and fentanyl-simulated interaction patterns confronted with experimental data. *Molecules* **25**(20), 4636. https://doi.org/10.3390/molecules25204636 (2020).

Author contributions

D.B., M.K and O.M. conceptualized and designed the project. J.W and O.M. developed methodology. D.B and S.B. acquired data. C.N.P and O.M analyzed and interpreted data. D.B., O.M and C.N.P. wrote manuscript. M.K and S.B. provided executive support. M.K. supervised the study. The whole manuscript was approved by all authors.

Declarations

Competing interests

The authors declare no competing interests.

Additional information

Supplementary Information The online version contains supplementary material available at https://doi.org/10.1038/s41598-025-96411-x.

Correspondence and requests for materials should be addressed to C.N.P.

Reprints and permissions information is available at www.nature.com/reprints.